

# Shielding Effectiveness of Some Hydrogenous Materials for Neutral Nuclear Radiations

K. S. Mann<sup>1,\*</sup>, AshaRani<sup>2</sup>, Manmohan Singh<sup>3</sup>, V. P. Singh<sup>4,\*</sup>, Turgay Korkut<sup>5</sup>

<sup>1</sup>Department of Applied Sciences, Punjab Technical University, Kapurthala-144601, India

<sup>2</sup>Department of Applied Sciences, Ferozpur College of Engineering and Technology, Ferozpur-142052, India

<sup>3</sup>Department of Physics, K.M.V. College, Jalandhar-144001, India

<sup>4</sup>Department of Physics, Karnatak University, Dharwad-580003, India

<sup>5</sup>Department of Nuclear Energy Engineering, Sinop University, Sinop-57000, Turkey

Received: 19 Mar. 2019, Revised: 20 Oct. 2019, Accepted: 11 Nov. 2019.

Published online: 1 Jan. 2020.

**Abstract:** Shielding effectiveness of six hydrogenous materials (polymer and plastic) for gamma and fast neutron are investigated using total mass attenuation coefficients, mass energy absorption coefficients, KERMA, effective atomic number, electron density and macroscopic effective removal cross-sections. The program WinXCOM for photons and mass removal cross section for individual elements for neutrons were used. It is found that increase of H-atom concentration leads to improve the neutron shielding and reduce gamma shielding effectiveness. Also, difference in effective mass removal cross-sections for elements using the theoretical computation and experiment was observed. Present investigation should be useful for application of these materials used in shielding in various nuclear facilities.

**Keywords:** Shielding, neutron, attenuation coefficient, energy absorption coefficient.

## 1 Introduction

The nuclear radiations are reported hazardous for living cells and tissues. For the safety point of view, a detailed study of adequate shielding material for the radiations is required. Nuclear and radioactive waste management is increasing demand in nuclear technology in several fields viz. nuclear-reactor, industry, medicine, agriculture, medical application and scientific research which grown significantly the gamma/neutron shielding development. The present investigation would be helpful for assessment of shielding effectiveness of some hydrogenous materials (H-atom containing) for neutral nuclear radiations (gamma and neutron).

Radiation shielding involves during placing a shielding material between the radiation source and receptors. Radiation is classified into two general groups, charged (alpha particles, beta particles) and uncharged (gamma and neutron). Charged particles are direct ionizing radiation whereas uncharged particles ionize by secondary radiation.

The charged particles have a limited range compared with uncharged particles. Therefore, the shielding of charged particles is comparatively easy than neutral radiations.

It is found that stopping neutron is very difficult because of high penetrating power, and it is attenuated by three major interaction processes viz. elastic scatter, inelastic scatter and absorption. The hydrogenous material attenuates neutron most effectively because of having similar order mass as proton. Similar to neutron, the gamma ray has a very high penetrating power. The first process of interaction of gamma is photo-electric effect in low energy region with high atomic number. The second interaction process is called Compton scattering, becomes dominant for gamma energies of above 0.1 MeV. In high energy region ( $> 1.02$  MeV), the pair-production becomes dominant.

Low cost and light weight shielding materials for neutral radiations is necessary for sustained development of the nuclear technology. Conventional radiation shielding materials such as lead, mercury and concrete are inconvenient because of high cost and toxicity. Water is being used as a shielding material as well as cooling in

\*Corresponding author - mail::ksmann6268@gmail.com

nuclear reactors. Water is found good neutron shielding material due to its high H-atom content. Similar to water, polymers and plastic materials are also rich in H-atom content. Therefore, shielding characterization of selected polymer and plastic materials are investigated.

Several researchers have investigated the gamma shielding characteristics of polymers, concretes, silicates and building materials [1,2,3,4,5]. Gamma and neutron attenuation coefficients for building materials [6,7, 8, 9 10, 11, 12], and compounds [13, 14]. The experimental values for fast neutron removal cross-sections of some boron compounds has been reported, also [15].

Aim of the present investigation is to characterise the H-rich materials for gamma and neutron shielding effectiveness using interaction parameters. Also, comparison mass removal cross-sections for elements using the theoretical computation and experiment methods. The results of present investigation should be useful for shielding application in various nuclear facilities and further investigation on neutron interactions.

## 2 Materials and Methods

The elemental compositions of the samples given in the Table 1 [16]. In these samples percentage concentration of H-atom (by weight) range is 2.47 to 10.20. The computation methods of interaction parameters have been used in the present investigation.

### 2.1 Effective Removal Cross-sections of Fast Neutrons

The effective removal cross-section is considered to be approximately constant for neutron energy range 2-12 MeV [17]. Experimentally calculated values of removal cross-section for different elements using the LTSF are available in ORNL-1843 report [18]. Some computer programs MERCSEF-N [19] and NXcom [20] have been developed for neutron and gamma of mixtures.

The total macroscopic cross-section,  $\Sigma_t$  is given as below [21,22,23]:

$$\Sigma_t = \frac{\rho N_a}{A} \sigma_t \quad (1)$$

Where  $\rho$  is the density ( $\text{g cm}^{-3}$ ),  $N_a$  is Avogadro's Number and  $A$  is the atomic mass.  $\Sigma_t$  has the dimensions of the inverse of the length; their unit is  $\text{cm}^{-1}$ . The attenuation of neutrons in matter follows the following law [21, 22, 23]:

$$I = I_0 e^{-\Sigma_t x} \quad (2)$$

Where  $I_0$  and  $I$  are respectively the intensities of neutrons unmitigated and mitigated,  $x$  (cm) is the thickness of the material medium and  $\Sigma_t$  represents the total macroscopic cross-section.

For fast neutron, macroscopic removal cross-section,  $\Sigma_R$  ( $\text{cm}^{-1}$ ) is given by the following formula [17, 24, 25, 26]:

$$\Sigma_R = \sum_i W_i (\Sigma_R / \rho)_i \quad (3)$$

Where  $W_i$ ,  $\rho$  and  $(\Sigma_R / \rho)_i$  and are the partial density ( $\text{g cm}^{-3}$ ), density and mass removal cross section of the  $i^{\text{th}}$  constituent, respectively. The values of  $(\Sigma_R / \rho)$  ( $\text{cm}^2 \text{g}^{-1}$ ) of all the elements which constitute the shielding materials

**Table 1:** Elemental composition of the hydrogenous samples (Hubbell and Seltzer, 2004).

Sample	Symbol	Density ( $\text{g/cm}^3$ )	Elemental composition (% by weight)
Bone-Equivalent Plastic (B-100)	S1	1.45	H(6.55),C(53.7),N(2.16),O(3.21),F(16.75),Ca(17.66)
Polyvinyl Chloride (PVC)	S2	1.41	H(4.84),C(38.44),Cl(56.73)
Air-equivalent Plastic (C-552)	S3	1.76	H(2.47),C(50.17),O(0.46),F(46.53),Si(0.40)
Radio chromic Dye Film (Nylon Base)	S4	1.08	H(10.20),C(65.44),N(9.89),O(14.47)
Polyethylene Terephthalate (Mylar)	S5	1.38	H(4.20),C(62.51),O(33.31)
Polymethyl Methacrylate (PMMA)	S6	1.19	H(8.06),C(59.99),O(31.97)

used in the present study were taken from literature [27, 17, 25, 26, 19, 14].

### 2.2 Total Mass Attenuation Coefficient

The exponential attenuation nature of photons are represented according to Lambert–Beer law as  $I = I_0 e^{-\mu x}$ . Where,  $I_0$  = initial dose rate,  $I$  = the shielded dose rate,  $\mu$  = linear attenuation coefficient in (cm<sup>-1</sup>) and  $x$  is the shield thickness in (cm). Total mass attenuation coefficient for gamma-ray photon ( $\mu_T$ ) can be calculated by using WinXCom computer software [28].

The theoretical values of total mass attenuation coefficient and mass energy-absorption coefficients have been calculated by using mixture rule, which can be found elsewhere literature.

### 2.3 KERMA Relative to Air

Kinetic energy released per unit mass (KERMA) has been connected with the mass energy absorption coefficient ( $\mu_{en}/\rho$ ) using the following relation [29, 6]:

$$K = \frac{\psi A (\mu_{en}) dx}{A dx} = \psi \left( \frac{\mu_{en}}{\rho} \right) \quad (4)$$

Where  $K$  represents KERMA and  $\psi$  be the energy fluence of mono-energetic photons passing normally through a cross-sectional area ‘ $A$ ’ in an interacting material. KERMA of samples relative to air can be expressed as  $K_R$ :

$$K_R = \frac{K_{Sample}}{K_{Air}} = \frac{\left( \frac{\mu_{en}}{\rho} \right)_{Sample}}{\left( \frac{\mu_{en}}{\rho} \right)_{Air}} \quad (5)$$

### 2.4 Effective Atomic Number and Electron Density

The  $(\mu_{en}/\rho)_{sample}$  values has been used to determine the total molecular absorption cross-section  $\sigma_m$  by the following relation:

$$\sigma_m = \frac{\sum_i n_i A_i \left( \frac{\mu_{en}}{\rho} \right)_{sample}}{N_A} \quad (6)$$

where  $n_i$  is the total number of atoms (with respect to mass number) in the molecule,  $A_i$  is the atomic weight of the  $i^{th}$  element in a molecule, and  $N_A$  is Avogadro’s number. The values of mass-energy absorption coefficients for about all the elements and some compounds were available in tabular form by Hubbell and Seltzer (1995).

The atomic attenuation cross-section  $\sigma_a$  can be obtained using the following equation:

$$\sigma_a = \frac{\left( \frac{\mu_{en}}{\rho} \right)_{sample}}{N_A \sum_i w_i / A_i} = \frac{\sum_i f_i A_i (\mu_{en} / \rho)_i}{N_A} = \frac{\sigma_m}{\sum_i n_i} \quad (7)$$

where  $f_i = n_i / \sum n_i$  is the fractional abundance of constituent element,  $n_i$  is the total number of atoms of the constituent element, and  $\sum n_i$  is the total number of atoms present in the molecular formula.

The electronic attenuation cross-section  $\sigma_e$  is given by:

$$\sigma_e = \frac{1}{N_A} \sum_i \frac{f_i A_i}{Z_i} \left( \frac{\mu_{en}}{\rho} \right)_i \quad (8)$$

where  $Z_i$  is the atomic number of constituent elements.

Finally, the photon energy absorption effective atomic number for photon energy absorption ( $Z_{PEA,eff}$ ) is given by:

$$Z_{PEA,eff} = \frac{\sigma_a}{\sigma_e} \quad (9)$$

The electron density (electron/g) can be derived using the following relation:

$$N_{el,eff} = \frac{\left( \frac{\mu_{en}}{\rho} \right)_{sample}}{\sigma_e} \quad (10)$$

### 2.5 Macroscopic Effective Removal Cross-Sections

A number of empirical expressions have been proposed for relating  $\Sigma_R$  (cm<sup>-1</sup>) to the atomic number  $Z$  or to the atomic mass  $A$  of the element in question. The accurate empirical expressions in use are [26]:

$$\sum_1 R / \rho = 0.21A^{-0.56} \text{ cm}^2 \text{ g}^{-1} \quad (11)$$

$$\sum_2 R / \rho = 0.00662A^{-1/3} + 0.33A^{-2/3} - 0.211A^{-1} \text{ cm}^2 \text{ g}^{-1} \quad (12)$$

(For  $A > 12$ )

$$\sum_3 R / \rho = 0.290Z^{-0.743} \text{ cm}^2 \text{ g}^{-1} \quad (\text{For } Z \leq 8) \quad (13)$$

$$\sum_4 R / \rho = 0.125Z^{-0.565} \text{ cm}^2 \text{ g}^{-1} \quad (\text{For } Z > 8) \quad (14)$$

$$\left\langle \sum R / \rho \right\rangle = \frac{\left( \sum_1 R / \rho + \sum_2 R / \rho + \sum_3 R / \rho + \sum_4 R / \rho \right)}{4} \quad (15)$$

Equations from (11)–(14) are restricted for elements of  $A$  and  $Z$  at certain numbers. The Eq. (15) gives the average value of macroscopic effective mass removal cross-sections ( $\Sigma_R/\rho$ ) for fast neutrons.

### 2.6 Standardization for Macroscopic Effective Removal Cross-Sections

Fig. 1 shows the comparison of the calculated values of

macroscopic effective mass removal cross-sections,  $\Sigma_R/\rho$  ( $\text{cm}^2 \text{g}^{-1}$ ) using Eq. (15), published literature values and experimental values of ORNL-1843 for elements with mass number (A) range (1.00794 to 238.02891). It is indicated that calculated values of macroscopic effective mass removal cross-sections differ very much from the experimental values but close to the published values. So we use the published values of macroscopic effective mass removal cross-sections,  $\Sigma_R/\rho$  ( $\text{cm}^2 \text{g}^{-1}$ ) for the present calculations effective removal cross-sections,  $\Sigma_R(\text{cm}^{-1})$  using Eq. (3).

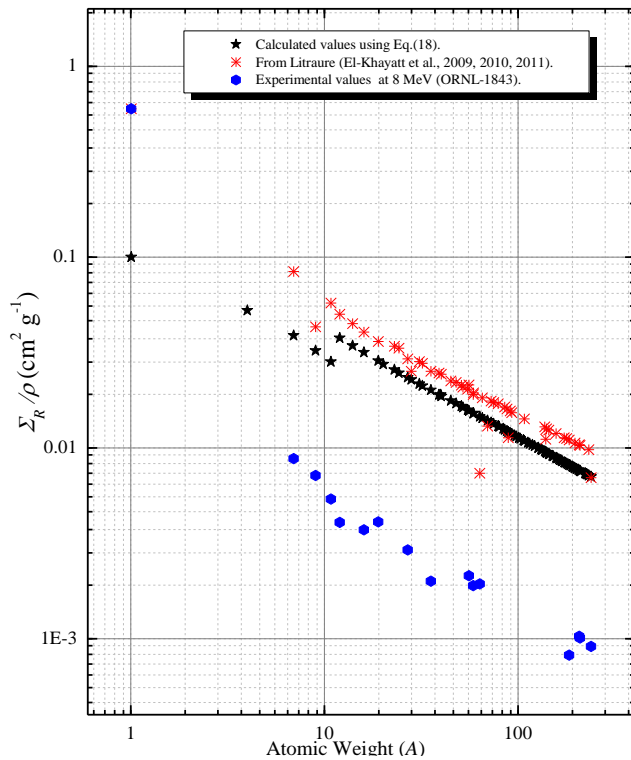


**Fig.1:** Comparison of the theoretical, experimental and published values of macroscopic effective mass removal cross-sections for elements with atomic weight (A).

### 3 Results and Discussion

#### 3.1 Gamma Radiations Shielding Characterization using Total Mass Attenuation and Mass Energy Absorption Coefficients

The mass attenuation coefficient of sample for gamma rays is a measure of the relative dominance of different interaction processes like photoelectric effect, Compton scattering and pair production. Figs. 2 and 3, clearly explain the variations of partial and total mass attenuation coefficients of the samples S2 and S4 with incident photon energies, we conclude from these figures that Photo electric absorption is dominating for photon energies below 50 keV and Compton scattering dominating for more than 50 keV in the selected samples. Also the total mass attenuation

coefficient is nearly equal to the Compton partial mass attenuation coefficient in the intermediate energy range (0.10- 1.4 MeV). Fig. 4 shows the variation of total mass attenuation coefficients of the samples. It is very clear that the maximum values of total mass attenuation coefficients are for sample S2 in energy range 0.01-0.1 MeV. The values of total mass attenuation coefficients are minimum for sample S4 for in energy range 0.01-0.02MeV but same for all samples in the energy range 0.02-12 MeV. Fig. 5 supports the above conclusions as the mass energy absorption coefficient values also follow the similar trend. Indicating S2 has highest ability to absorb incident photons in energy range 0.01-0.02 MeV.

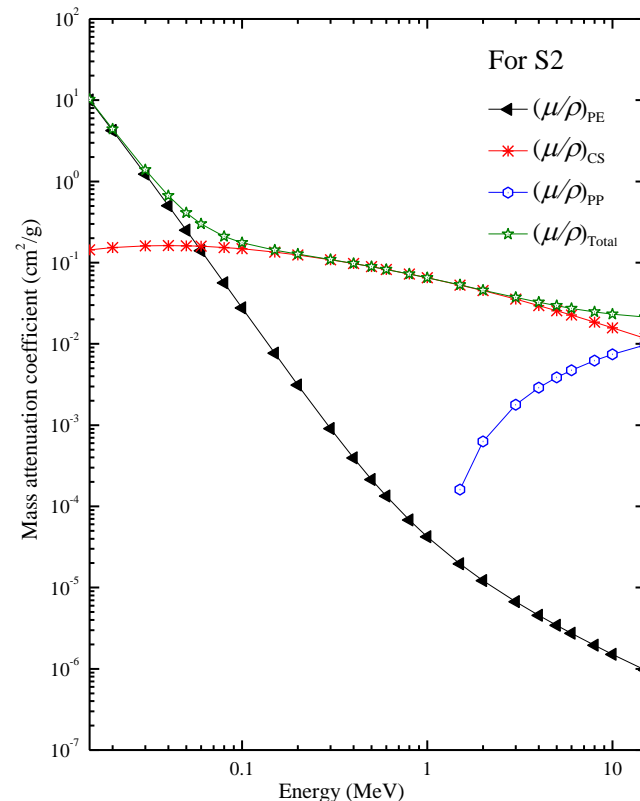


**Fig.2:** Variation of partial and total mass attenuation coefficients with incident photon energies for sample S2.

#### 3.2 Gamma Radiations Shielding Characterization Using KERMA

Fig. 6 shows the variation of KERMA of samples relative to air. It is evident from the figure that sample S3 seems the most equivalent to air as for S3 the value of  $K_R$  is close to unity for the entire selected energy range. So sample S3 has been found to be a material equivalent to air for the ionizing radiations in the selected energy range. The samples S1 and S2 have KERMA more than air in energy range 0.01-0.02 MeV verifying the higher abilities to absorb photons than air and other samples in the study.

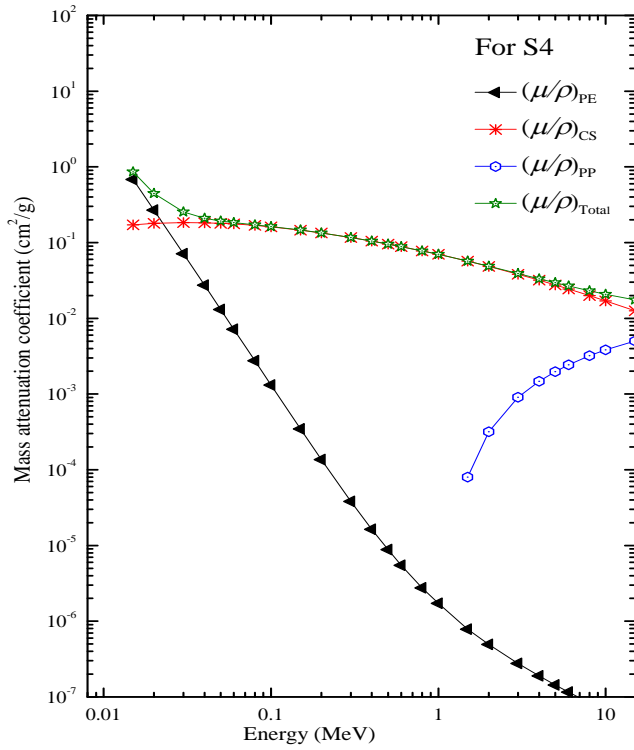


**Fig. 3:** Variation of partial and total mass attenuation coefficients with incident photon energies for sample S4.

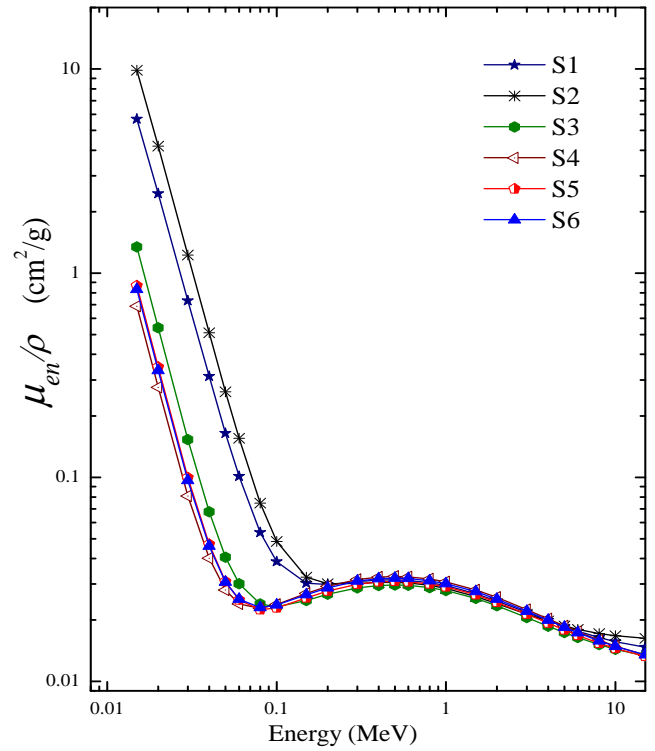


**Fig. 5:** Assessment of total mass energy absorption coefficients of all the samples in the chosen energy range.

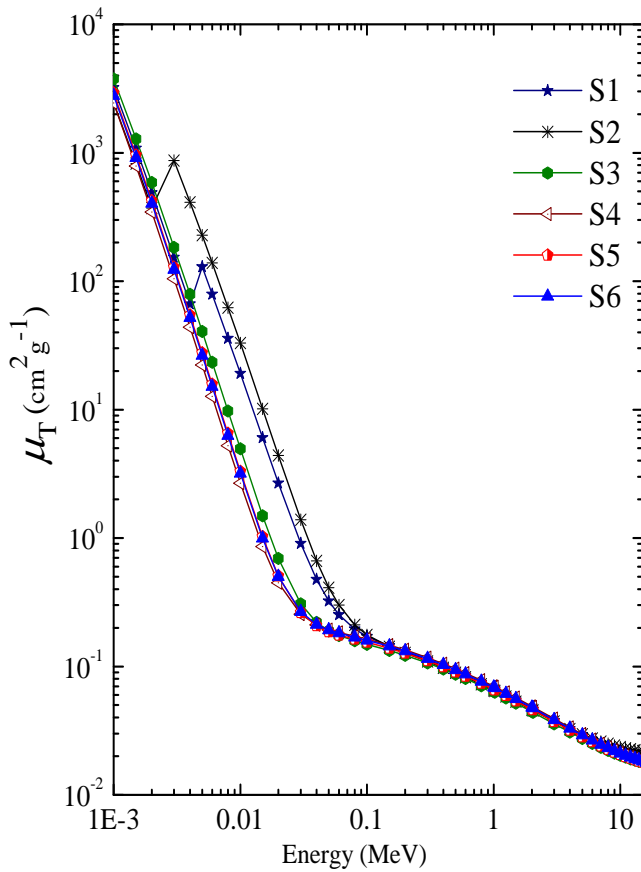


**Fig. 4:** Comparison of total mass attenuation coefficients for all the samples in the chosen energy range.

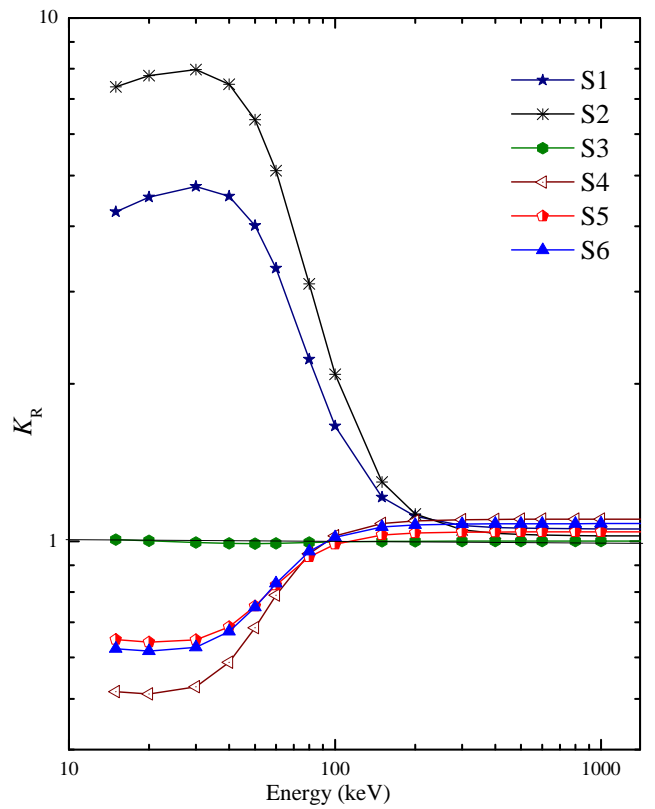


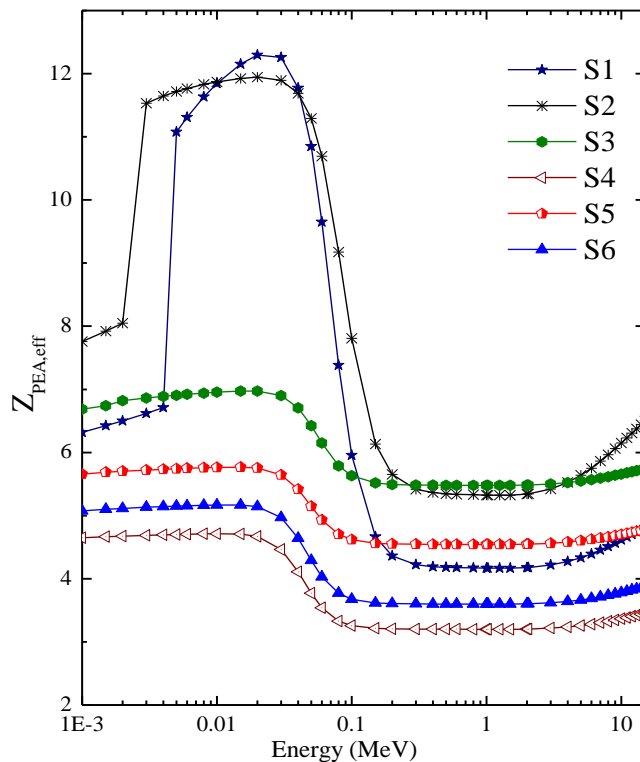
**Fig. 6:** KERMA relative to air for all samples in the selected energy range.



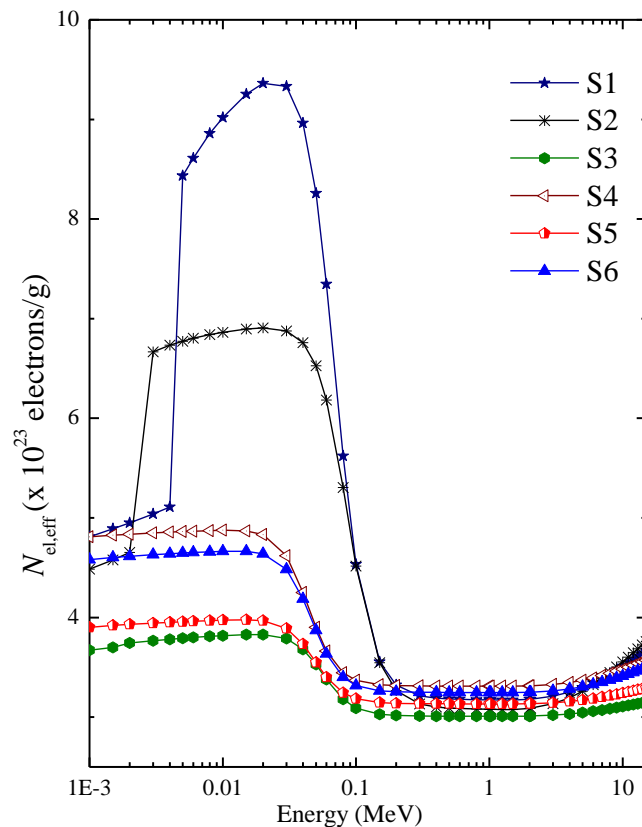
### 3.3 Gamma Radiation Shielding Dependence on Effective Atomic Number and Electron Density

Fig. 7 shows that S2 has maximum and S4 has minimum values of  $Z_{PEA,eff}$  in the energy range 0.001-0.200 MeV. The shielding character of a sample depends directly on the value of  $Z_{PEA,eff}$ . So, S2 seems to be the best and S4 seems the worst sample for shielding of neutral radiations in the lower part of the selected energy range. Sample S3 seems to be the best shielding material for gamma rays in the energy range 0.30-4.00 MeV.

The variation in effective electron density ( $N_{el,eff}$ ) with incident photon energy is shown in Fig.8, follows the same trend as observed for the photon energy absorption effective atomic number. Under the dominance of any photon interaction, electron density remains constant for a particular sample and the value for electron density varies significantly, whenever there is a shift of dominance from one process to the other. High value of electron density (computed in the units of electron/g) means the presence of more number of electrons per unit mass and hence more probability of photon interaction with these electrons, which in turn means the transfer of photon energy to the electrons or energy deposited to the material (as the penetration of electrons through thick volumes of the material is very less).



**Fig. 7:** Variations of effective atomic numbers for all samples in chosen energy range.



**Fig. 8:** Variations of effective electron densities for all samples in chosen energy range.

### 4.4. Neutron Shielding Characterization using Macroscopic Effective Removal Cross-Sections for Fast Neutrons $\Sigma_R$ ( $cm^{-1}$ )

The elemental compositions of the samples as fraction by weight (FBW), partial density (PD) and calculated values of effective fast neutron removal cross sections  $\Sigma_R$  ( $cm^{-1}$ ) using Eq. (14) for the selected samples have been listed in the Table 2a,b. These calculated values are applicable for neutron energy range of 2-12 MeV. It is observed that the total removal cross section is the maximum for S1 and minimum for S2, this lead to the conclusion that the S1 is more effective for neutron attenuation than other samples. The low variation in removal cross section is being noticed for all samples. Elevated values of removal cross section of S1 and S4 is attributed due to high density and large contribution of low atomic number weight fractions of H and C. With constant H weight fraction and variable densities, the removal cross section varies. In cases of S4, the removal cross section is slightly higher due to large C weight fraction. Therefore it is concluded that low atomic number elemental composition and density contribute a vital role in neutron shielding properties of the material. Figs. 9 and 10 shows that S1 is the best and S2 is worst sample for shielding of neutrons in the energy range 2-12 MeV.

**Table 2a.** Fast neutron removal cross section of the samples in energy range of 2-12 MeV.

Elements	S1			S2			S3
	$\rho : 1.45 \text{ gcm}^{-3}$			$\rho : 1.41 \text{ gcm}^{-3}$			$\rho : 1.76 \text{ gcm}^{-3}$
	FBW	PD	$\Sigma_R(\text{cm}^{-1})$	FBW	PD	$\Sigma_R(\text{cm}^{-1})$	FBW
H	0.0655	0.0949	0.0568	0.0484	0.0682	0.0408	0.0247
C	0.5369	0.7786	0.0391	0.3844	0.5419	0.0272	0.5016
N	0.0215	0.0312	0.0014	0.0000	0.0000	0.0000	0.0000
O	0.0321	0.0465	0.0019	0.0000	0.0000	0.0000	0.0045
F	0.1674	0.2428	0.0088	0.0000	0.0000	0.0000	0.4652
Si	0.0000	0.0000	0.0000	0.0000	0.0000	0.0000	0.0040
Cl	0.0000	0.0000	0.0000	0.5673	0.7998	0.0202	0.0000
Ca	0.1766	0.2560	0.0062	0.0000	0.0000	0.0000	0.0000
<b>Total</b>	<b>1.0000</b>	<b>1.4500</b>	<b>0.1141</b>	<b>1.0000</b>	<b>1.4100</b>	<b>0.0882</b>	<b>1.0000</b>

PD: Partial density.

FBW: Fraction by weight.

**Table 2b.** Fast neutron removal cross section of the samples in energy range of 2-12 MeV.

Elements	S4			S5			S6		
	$\rho : 1.08 \text{ gcm}^{-3}$			$\rho : 1.38 \text{ gcm}^{-3}$			$\rho : 1.19 \text{ gcm}^{-3}$		
	FBW	PD	$\Sigma_R(\text{cm}^{-1})$	FBW	PD	$\Sigma_R(\text{cm}^{-1})$	FBW	PD	$\Sigma_R(\text{cm}^{-1})$
H	0.1020	0.1102	0.0659	0.0420	0.0579	0.0346	0.0805	0.0958	0.0573
C	0.6544	0.7067	0.0355	0.6250	0.8625	0.0433	0.5998	0.7138	0.0358
N	0.0989	0.1068	0.0048	0.0000	0.0000	0.0000	0.0000	0.0000	0.0000
O	0.1447	0.1563	0.0063	0.3330	0.4596	0.0186	0.3196	0.3803	0.0154
F	0.0000	0.0000	0.0000	0.0000	0.0000	0.0000	0.0000	0.0000	0.0000
Si	0.0000	0.0000	0.0000	0.0000	0.0000	0.0000	0.0000	0.0000	0.0000
Cl	0.0000	0.0000	0.0000	0.0000	0.0000	0.0000	0.0000	0.0000	0.0000

Ca	0.0000	0.0000	0.0000	0.0000	0.0000	0.0000	0.0000	0.0000	0.0000
<b>Total</b>	<b>1.0000</b>	<b>1.0800</b>	<b>0.1125</b>	<b>1.0000</b>	<b>1.3800</b>	<b>0.0965</b>	<b>1.0000</b>	<b>1.1900</b>	<b>0.1086</b>

PD: Partial density.

FBW: Fraction by weight.

**Table 3.** Atomic cross section ( $\sigma_a$ ) in Barns.

Energy (MeV)	S1	S2	S3	S4	S5	S6
0.0150	74.7478	170.5497	24.5066	6.6602	12.5710	9.2236
0.0200	32.1911	72.4086	9.8506	2.6631	5.0219	3.6888
0.0300	9.6261	21.1973	2.7882	0.7837	1.4461	1.0688
0.0400	4.0968	8.8328	1.2346	0.3879	0.6809	0.5096
0.0500	2.1607	4.5316	0.7394	0.2708	0.4470	0.3399
0.0600	1.3291	2.6866	0.5492	0.2320	0.3637	0.2803
0.0800	0.7044	1.2921	0.4362	0.2202	0.3259	0.2552
0.1000	0.5069	0.8385	0.4225	0.2301	0.3331	0.2624
0.1500	0.3979	0.5601	0.4545	0.2611	0.3724	0.2945
0.2000	0.3918	0.5214	0.4869	0.2827	0.4021	0.3183
0.3000	0.4046	0.5228	0.5236	0.3054	0.4338	0.3436
0.4000	0.4118	0.5284	0.5377	0.3139	0.4457	0.3530
0.5000	0.4130	0.5287	0.5409	0.3159	0.4486	0.3553
0.6000	0.4105	0.5250	0.5384	0.3145	0.4466	0.3537
0.8000	0.4002	0.5113	0.5255	0.3071	0.4359	0.3453
1.0000	0.3870	0.4942	0.5085	0.2972	0.4219	0.3342
1.0220	0.3853	0.4920	0.5063	0.2959	0.4201	0.3327
1.2500	0.3697	0.4720	0.4860	0.2840	0.4032	0.3194
1.5000	0.3534	0.4511	0.4646	0.2715	0.3854	0.3053
2.0000	0.3254	0.4164	0.4274	0.2495	0.3544	0.2807
2.0440	0.3232	0.4137	0.4244	0.2477	0.3519	0.2786
3.0000	0.2863	0.3700	0.3747	0.2175	0.3098	0.2450
4.0000	0.2610	0.3419	0.3400	0.1959	0.2800	0.2210
5.0000	0.2438	0.3238	0.3161	0.1806	0.2592	0.2043
6.0000	0.2315	0.3116	0.2988	0.1693	0.2439	0.1919
7.0000	0.2227	0.3036	0.2862	0.1608	0.2327	0.1826
8.0000	0.2155	0.2971	0.2758	0.1538	0.2234	0.1751
9.0000	0.2103	0.2931	0.2683	0.1485	0.2165	0.1693
10.0000	0.2058	0.2895	0.2616	0.1439	0.2104	0.1643
11.0000	0.2026	0.2875	0.2570	0.1404	0.2061	0.1607
12.0000	0.1998	0.2858	0.2530	0.1374	0.2022	0.1575



**Table 4.** Electronic cross section ( $\sigma_{el}$ ) in Barns.

Energy (MeV)	S1	S2	S3	S4	S5	S6
0.0150	6.1508	14.3003	3.5136	1.4152	2.1794	1.7847
0.0200	2.6179	6.0617	1.4124	0.5702	0.8728	0.7175
0.0300	0.7853	1.7823	0.4041	0.1755	0.2562	0.2151
0.0400	0.3480	0.7556	0.1841	0.0944	0.1258	0.1099
0.0500	0.1992	0.4014	0.1151	0.0718	0.0868	0.0793
0.0600	0.1377	0.2513	0.0893	0.0655	0.0737	0.0696
0.0800	0.0954	0.1408	0.0753	0.0661	0.0693	0.0677
0.1000	0.0851	0.1074	0.0750	0.0706	0.0721	0.0714
0.1500	0.0853	0.0913	0.0824	0.0812	0.0816	0.0814
0.2000	0.0898	0.0923	0.0886	0.0882	0.0883	0.0883
0.3000	0.0958	0.0965	0.0955	0.0954	0.0954	0.0954
0.4000	0.0983	0.0985	0.0981	0.0981	0.0981	0.0981
0.5000	0.0988	0.0989	0.0987	0.0987	0.0987	0.0987
0.6000	0.0983	0.0984	0.0982	0.0983	0.0983	0.0983
0.8000	0.0959	0.0959	0.0959	0.0960	0.0959	0.0960
1.0000	0.0928	0.0928	0.0928	0.0929	0.0928	0.0929
1.0220	0.0924	0.0924	0.0924	0.0925	0.0924	0.0925
1.2500	0.0887	0.0887	0.0887	0.0888	0.0887	0.0888
1.5000	0.0848	0.0847	0.0848	0.0848	0.0848	0.0848
2.0000	0.0779	0.0780	0.0780	0.0779	0.0779	0.0779
2.0440	0.0774	0.0774	0.0774	0.0773	0.0774	0.0773
3.0000	0.0679	0.0683	0.0681	0.0676	0.0679	0.0677
4.0000	0.0611	0.0619	0.0616	0.0605	0.0611	0.0607
5.0000	0.0563	0.0574	0.0570	0.0554	0.0563	0.0558
6.0000	0.0527	0.0542	0.0536	0.0516	0.0528	0.0520
7.0000	0.0500	0.0518	0.0512	0.0487	0.0501	0.0492
8.0000	0.0478	0.0498	0.0491	0.0463	0.0479	0.0469
9.0000	0.0461	0.0484	0.0476	0.0444	0.0462	0.0450
10.0000	0.0446	0.0471	0.0462	0.0428	0.0448	0.0435
11.0000	0.0435	0.0461	0.0453	0.0415	0.0437	0.0423
12.0000	0.0425	0.0453	0.0444	0.0404	0.0427	0.0412

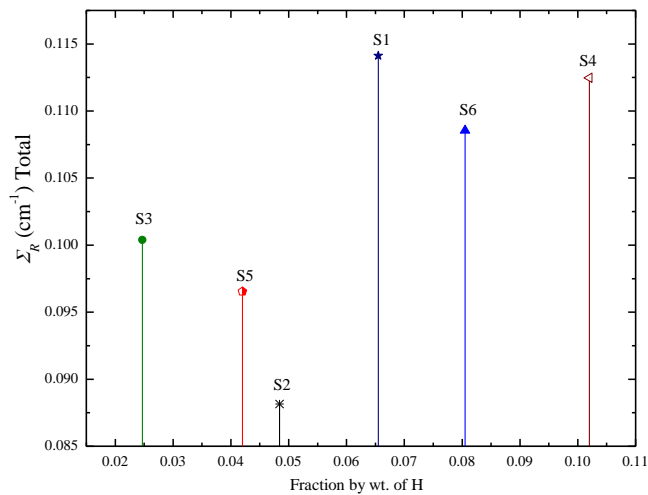


**Fig. 9:** Comparison of total effective removal cross sections for fast neutrons with H-fraction by weights of all samples.

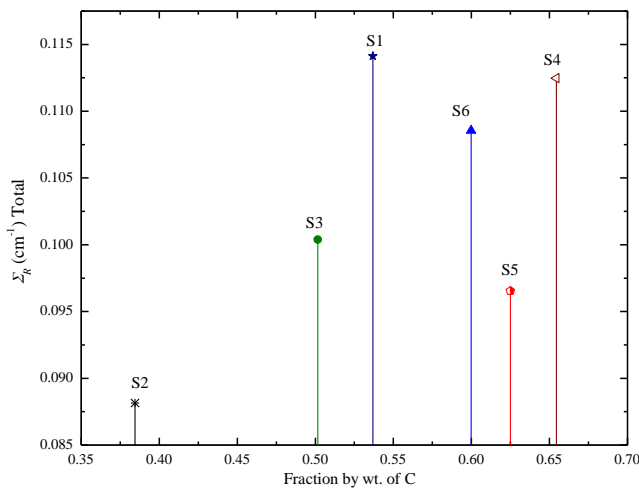


**Fig. 10:** Comparison of total effective removal cross sections for fast neutrons with C-fraction by weights of all samples.

## 4 Conclusions

We have concluded some useful results as follows;

- The same material cannot be used for effective shielding of both nuclear neutral radiations (x-rays & gamma-rays) and neutrons. As S2 seems to have good shielding property for neutral radiations (10-1400 keV) and worst for fast neutrons (2-12 MeV).
- Low-Z composition and density contribute a vital role in neutral radiations and neutron shielding properties. A good correlation has been seen in the neutral radiations interaction parameters of the samples.
- Different interaction parameters used in the investigation strongly dependent on the elemental composition of the sample in the lower energy region (dominant region of photoelectric effect), whereas in

the intermediate energy region, the dependence on elemental composition becomes very weak due to dominance of Compton scattering.

## Acknowledgement

We are grateful to respected Dr. A.M. El-Khayatt, Dr. M.J. Berger and Prof. Dr. L. Gerward for providing the WinXCom program, helping and guiding us for computation for this work. Authors paid a tribute to respected Late Dr. J.H. Hubbell for his valuable contribution in the field of theoretical nuclear physics.

## References

- [1] Kurudirek, M., Turkmen, I., Ozdemir, Y., A study of photon interaction in some building materials: high-volume admixture of blast furnace slag into Portland cement. *Radiat. Phys. Chem.*, **78**, 751-759 (2009).
- [2] Akkurt, İ., Akyildirim, H., Mavi, B., Kilincarslan, S., Basyigit, C., Photon attenuation coefficients of concrete includes barite in different rate. *Ann. Nucl. Energy.*, **37-7**, 910-914 (2010).
- [3] Akkurt, İ., Akyildirim, H., Mavi, B., Kilincarslan, S., Basyigit, C., Gamma-ray shielding properties of concrete including barite at different energies. *Prog. Nucl. Energy.*, **52**, 620-623, 2010.
- [4] Damla, N., Cevik, U., Kobya, A.I., Celik, A., Celik, N., Van Grieken, R., Radiation dose estimation and mass attenuation coefficients of cement samples used in Turkey. *J. Hazard. Mater.*, **176**, 644-649, 2010.
- [5] Turkmen, İ., Özdemir, Y., Kurudirek, M., Demir, F., Simsek, Ö., Demirbog, R., Calculation of radiation attenuation coefficients in Portland cements mixed with silica fume, blast furnace slag and natural zeolite. *Ann. Nucl. Energy.*, **35**, 1937-1943, 2008.
- [6] Singh, T., Rajni, Kaur, U., Singh, P.S., Photon energy absorption parameters for some polymers. *Ann. Nucl. Energy.*, **37**, 422-427, 2010.
- [7] Akkurt, İ., El-Khayatt, A.M., The effect of barite proportion on neutron and gamma-ray shielding. *Ann. Nucl. Energy.*, **51**, 5-9, 2013.
- [8] Yilmaz, E., Baltas, H., Kirisa, E., Ustabas, İ., Cevik, U., El-Khayatt, A.M., Gamma-ray and neutron shielding properties of some concrete materials. *Ann. Nucl. Energy.*, **38(10)**, 2204-2212, 2011.
- [9] Osman, Gencel, Ahmet, Bozkurt, Erol, Kamc, Turgay, Korkut, Determination and calculation of gamma and neutron shielding characteristics of concretes containing different hematite proportions. *Ann. Nucl. Energy.*, **38**, 2719-2723, 2011.
- [10] Mann, K.S., Kurudirek, M., Sidhu, G.S., Verification of dosimetric materials to be used as tissue-substitutes in radiological diagnosis. *Appl. Radiat. Isot.*, **70**, 681-691, 2012
- [11] Mann, K.S., Sidhu, G.S., Verification of some low-Z silicates as gamma-ray shielding materials. *Ann. Nucl. Energy.*, **40**, 241-252, 2012.
- [12] Mann, K.S., Korkut, T., Gamma-ray buildup factors study for deep penetration in some silicates. *Ann. Nucl. Energy.*, **51**, 81-93, 2013

- [13] Kurudirek, M., Ozdemir, Y., Energy absorption and exposure buildup factors for some polymers and tissue substitute materials: photon energy, penetration depth and chemical composition dependence. *J. Radiol. Prot.*, **31**, 117–128, 2011.
- [14] El-Khayatt, A.M., Radiation shielding of concretes containing different lime/ silica ratios. *Ann. Nucl. Energy.*, **37(7)**, 991–995, 2010.
- [15] Korkut, T., Karabulut, A., Budak, G., Korkut, H., Investigation of fast neutron shielding characteristics depending on boron percentages of MgB<sub>2</sub>, NaBH<sub>4</sub> and KBH<sub>4</sub>. *J. Radioanal. Nucl. Chem.*, **286**, 61–65, 2010.
- [16] Hubbell, J.H. and Seltzer, S.M., Tables of X-Ray mass attenuation coefficients and mass energy-absorption coefficients from 1 keV to 20 MeV for elements Z = 1 to 92 and 48 additional substances of dosimetric interest. NISTIR-5632, Gaithersburg, MD., 2004.
- [17] Kaplan, M.F., Concrete Radiation Shielding. John Wiley & Sons, New York., 1989.
- [18] Chapman, G. T., Störns, C. L., Effective neutron removal cross sections for shielding using LTSF, AEC research and development report- ORNL-1843 special, Tennessee, 1955.
- [19] El-Khayatt, A.M., El-Sayed Abdo, A., MERCSF-N calculation program for fast neutron removal cross-sections in composite shields. *Ann Nucl Energy.*, **36(6)**, 832–836, 2009.
- [20] El-Khayatt, A.M., NXcom – a program for calculating attenuation coefficients of fast neutrons and gamma-rays. *Ann. Nucl. Energy.*, **38(1)**, 128–132, 2011.
- [21] Shultis, J.K., Faw, R.E., Radiation Shielding. Prentice Hall, New York, 1996.
- [22] Shultis, J.K., Faw, R.E., Fundamentals of Nuclear Science and Engineering 2nd ed. CRC Press, Boca Raton, FL, 2008.
- [23] Martin, J.E., Physics for Radiation Protection. Wiley, New York, 2000
- [24] Glasstone, S., Sesonske, A., Nuclear Reactor Engineering, third ed. CBS Publishers & Distributors, Shahdara, Delhi, India, 1986.
- [25] Profio, A.E., Radiation Shielding and Dosimetry. Wiley, New York, 1979.
- [26] Wood, J., Computational Methods in Reactor Shielding. Pergamon Press, New York, 1982.
- [27] Chilton, A.B., Shultis, J.K., Faw, R.E., Principles of Radiation Shielding, Prentice- Hall, New York, 1984.
- [28] Gerward, L., Guilbert, N., Jensen, K.B., Levring, H., WinXCom – A program for calculating X-ray attenuation coefficients. *Radiat. Phys. Chem.*, **71**, 653–654, 2004.
- [29] Manohara, S.R., Hanagodimath, S.M., Gerward, L., Studies on effective atomic number, electron density and kerma for some fatty acids and carbohydrates. *Phys. Med. Biol.*, **53**, 377-386, 2008.